

Neutron Diffraction and Neutron Vibrational Spectroscopy Studies of Hydrogen Adsorption in the Prussian Blue Analogue $\text{Cu}_3[\text{Co}(\text{CN})_6]_2$

Michael R. Hartman,* Vanessa K. Peterson, and Yun Liu

NIST Center for Neutron Research, National Institute of Standards and Technology, 100 Bureau Drive, MS 8562, Gaithersburg, Maryland 20899-8562

Steven S. Kaye and Jeffrey R. Long

Department of Chemistry, University of California, Berkeley, California 94720-1460

Received April 13, 2006

The adsorption of molecular hydrogen in the Prussian blue analogue $\text{Cu}_3[\text{Co}(\text{CN})_6]_2$ was investigated using high-resolution neutron powder diffraction and neutron vibrational spectroscopy. Rietveld structural refinement of the neutron data for hydrogen loadings of 1, 2, and $\sim 2.3 \text{ H}_2/\text{Cu}$ showed that the hydrogen was adsorbed at two sites within the structure. The most prominent adsorption site, located at the $(1/4, 1/4, 1/4)$ crystallographic site, was an interstitial location within the structure. The second adsorption site was associated with exposed Cu^{2+} ion coordination sites that result from the presence of $[\text{Co}(\text{CN})_6]^{3-}$ vacancies within the structure of the material. The rotational–vibrational density of states of the adsorbed hydrogen was probed using neutron vibrational spectroscopy and showed a range of local binding potentials for the adsorbed hydrogen.

Introduction

The transition to an energy infrastructure based upon hydrogen as an energy carrier is critically dependent upon the successful development of a safe, efficient, and compact means to store hydrogen, particularly for transportation applications. Solid-state storage of hydrogen shows promise because of its ability to achieve high volumetric and gravimetric storage densities. One prototype class of solid-state material capable of adsorbing molecular hydrogen is the Prussian blue analogues $\text{M}_3[\text{M}'(\text{CN})_6]_2$, where M is a divalent metal and M' is a trivalent metal.^{1,2} Within the $\text{M}_3[\text{M}'(\text{CN})_6]_2$ structure, only 2/3 of the $[\text{M}'(\text{CN})_6]^{3-}$ atomic sites are occupied to achieve the correct charge balance with the face-centered cubic framework of M atoms. The $[\text{M}'(\text{CN})_6]^{3-}$ vacancies result in an aperiodic system of nanoporous voids throughout the material, which nominally contain water adsorbed to the uncoordinated M atoms. However, removal of this adsorbed water is possible, which leads to a nanoporous framework structure in which gas adsorption might occur both within interstitial crystalline sites as well as at exposed metal coordination sites.

In a recent study, the hydrogen adsorption properties of various Prussian blue analogues were investigated with the highest gravimetric storage density observed for $\text{Cu}_3[\text{Co}(\text{CN})_6]_2$ at 1.8 wt % (77 K, 1 bar).¹ Further optimization of these materials might be possible if the exact nature of the hydrogen adsorption could be more fully understood.

In the present study, we report the results of a neutron powder diffraction investigation of a Prussian blue analogue $\text{Cu}_3[\text{Co}(\text{CN})_6]_2$ with varying amounts of adsorbed hydrogen. In addition, neutron vibrational spectroscopy was used to probe the local binding environment of the adsorbed hydrogen by monitoring changes in the rotational–vibrational spectrum associated with the adsorbed hydrogen.

Experimental Section

The synthesis and characterization of the Prussian blue analogue $\text{Cu}_3[\text{Co}(\text{CN})_6]_2$ used throughout this investigation have been reported elsewhere.¹ Water adsorbed in the pores of the structure was removed prior to the adsorption of hydrogen by heating the sample under dynamic vacuum at a rate of 1 K/min from room temperature to 368 K where the sample was maintained for a period of 48 h.

For the neutron powder diffraction studies, the $\text{Cu}_3[\text{Co}(\text{CN})_6]_2$ was loaded into a vanadium can sealed with a lead gasket. The sample can was equipped with a capillary line that allowed the transfer of hydrogen into and out of the sample. The sample assembly was then loaded into a closed-cycle helium refrigerator which was used to control temperatures throughout the measurement. To ensure that hydrogen did not condense in the capillary tubing, the sample was warmed to 77 K prior to gas loading. With the sample at 77 K, hydrogen was charged into the sample by filling an external control volume of known volume and temperature to a predetermined hydrogen pressure. A valve connecting the control volume to the sample assembly was then opened, allowing hydrogen to interact with the sample. The state of the hydrogen adsorption was followed by monitoring pressure in the control volume. For loadings approaching the saturated hydrogen loading, it was necessary to cool the sample further (to $\sim 30 \text{ K}$) to get all of the hydrogen adsorbed onto the structure. Once the adsorption process

* To whom correspondence should be addressed. E-mail: michael.hartman@nist.gov.

(1) Kaye, S. S.; Long, J. R. *J. Am. Chem. Soc.* **2005**, *127*, 6507.

(2) Chapman, K. W.; Southon, P. D.; Weeks, C. L.; Kepert, C. J. *Chem. Commun.* **2005**, 3322.

Table 1. Summary of Rietveld Refinement of Evacuated $\text{Cu}_3[\text{Co}(\text{CN})_6]_2$

space group	$Fm\bar{3}m$				
sample temperature [K]	3.5				
lattice parameter [\AA]	10.0003(3)				
R_{wp}	0.0568				
R_{p}	0.0461				
DWd	1.221				
atom	x	y	z	fractional occupation	U_{iso}
Cu	1/2	0	0	1	0.061(7)
Co	0	0	0	2/3	0.034(11)
C	0.1890(9)	0	0	2/3	0.039(3)
N	0.3030(7)	0	0	2/3	0.042(2)

was complete, the sample was cooled further to ~ 5 K to minimize thermal motion and permit a more accurate structural determination. Neutron powder diffraction data were collected on the high-resolution neutron powder diffractometer BT-1 at the NIST Center for Neutron Research (NCNR) using neutrons with a wavelength of 1.5403 \AA . Diffraction data for the various hydrogen loadings were subjected to Rietveld refinement using the GSAS computer code as implemented in EXPGUI.^{3,4} Neutron powder diffraction patterns were measured for the evacuated material as well as with hydrogen loadings of 1, 2, and ~ 2.3 H_2/Cu atom.⁵ For the highest loading, some of the admitted gas would not adsorb to the structure and had to be pumped out, which resulted in a loading of ~ 2.3 H_2/Cu .

The rotational–vibrational density of states of the adsorbed hydrogen was studied using the filter analyzer neutron spectrometer (FANS) at the NCNR.⁶ In this measurement, the $\text{Cu}_3[\text{Co}(\text{CN})_6]_2$ was loaded into an aluminum sample cell, equipped with a gas handling line, and sealed with a lead gasket. The sample assembly was again loaded into a closed-cycle helium refrigerator and cooled to ~ 5 K. Hydrogen was admitted to the sample in the manner described above. Measurements were taken at several different hydrogen loadings so that the changes in the spectrum could be observed as the adsorbed hydrogen populated different adsorption sites throughout the structure.

Results and Discussion

Initially, the diffraction data from the evacuated $\text{Cu}_3[\text{Co}(\text{CN})_6]_2$ were subjected to a Rietveld refinement, refining the scale, lattice, background, peak profile, atomic position, and isotropic atomic displacement parameters. The Rietveld refinement was performed in the $Fm\bar{3}m$ space group, and the $\text{Cu}_3[\text{Co}(\text{CN})_6]_2$ lattice parameter at 3.5 K was 10.0003(3) \AA . The resulting structural model, summarized in Table 1, was used as the starting model for the analysis of the powder diffraction data for a hydrogen loading of 1 H_2/Cu . After equilibrating the structural model by allowing changes in the scale, lattice, and background parameters, a difference Fourier technique was used to isolate the unaccounted for scattering length density associated with the adsorbed hydrogen. The results of the difference Fourier analysis are

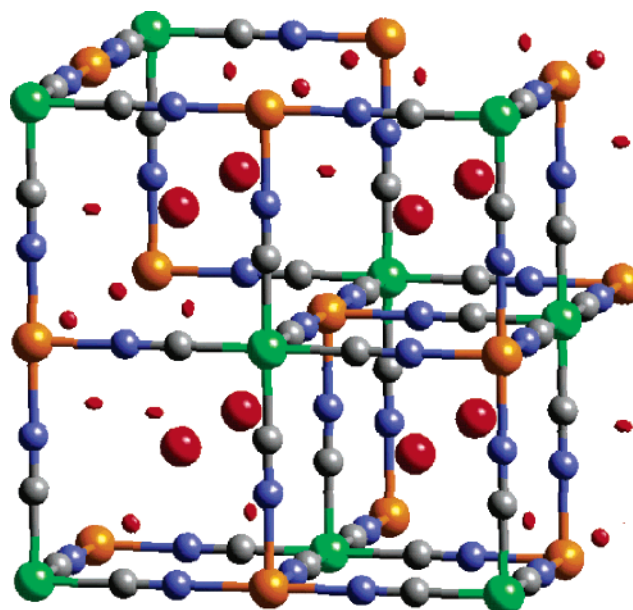


Figure 1. Results of the difference Fourier analysis for a hydrogen loading of 1 H_2/Cu , showing the unaccounted for scattering length density (red) superimposed on the unit cell of $\text{Cu}_3[\text{Co}(\text{CN})_6]_2$. The atom designations are copper (orange), cobalt (green), carbon (gray), and nitrogen (blue). Note that some of the $[\text{Co}(\text{CN})_6]^{3-}$ have been removed to simulate vacancies present in the actual material.

shown in Figure 1, where it was observed that the hydrogen adsorption occurs at two crystallographic locations, the $(\frac{1}{4}, \frac{1}{4}, \frac{1}{4})$ sites as well as an $(x, 0, 0)$ site where $x \approx 0.184$. The $(\frac{1}{4}, \frac{1}{4}, \frac{1}{4})$ site was the preferred adsorption site, accounting for $\sim 75\%$ of the hydrogen adsorbed at this loading. Hydrogen molecules were included at the two adsorption sites, and a more thorough Rietveld refinement was conducted, allowing for refinement of scale, lattice, background, peak profile, atomic position, and isotropic atomic displacement parameters. In addition, the fractional occupation parameters of the hydrogen atoms were refined to account for partial occupation of the adsorption sites. The results of the Rietveld fitting procedure for a hydrogen loading of 1 H_2/Cu are shown in Figure 2. The background oscillations are the result of diffuse scattering from the $[\text{Co}(\text{CN})_6]^{3-}$ vacancies and possibly from the presence of a small amount of amorphous material in the sample as a result of framework collapse during the evacuation process.⁷

The diffraction data for the additional hydrogen loadings were analyzed in an analogous manner, using the crystal structure model from the prior H_2 loading in conjunction with a difference Fourier analysis. The Rietveld refinements of the additional hydrogen loadings were of comparable quality to that shown in Figure 2, and no additional adsorption sites, beyond the two already indicated, were found. The results from the Rietveld refinements at all H_2 loadings are summarized in Table 2. The specific details for the hydrogen adsorption sites are listed in Table 3. As shown in Table 2, the crystalline lattice expands slightly to accommodate the hydrogen adsorption. The expansion is more pronounced for the higher hydrogen loadings, where the majority of the

(3) Larson, A. C.; Von Dreele, R. B. *General Structure Analysis System (GSAS)*; Report LAUR 86-748; Los Alamos National Laboratory: Los Alamos, NM, 2000.

(4) Toby, B. H. *J. Appl. Crystallogr.* **2001**, *34*, 210.

(5) For the neutron powder diffraction experiments, hydrogen gas enriched in deuterium (99.9% D) was used instead of hydrogen gas with the normal isotopic ratio to eliminate the large incoherent scattering associated with hydrogen.

(6) Udovic, T. J.; Neumann, D. A.; Leão, J.; Brown, C. M. *Nucl. Instrum. Methods Phys. Res., A* **2004**, *517*, 189.

(7) Franz, P.; Ambrus, C.; Hauser, A.; Chernyshov, D.; Hostettler, M.; Hauser, J.; Keller, L.; Krämer, K.; Stoeckli-Evans, H.; Pattison, P.; Bürgi, H.-B.; Decurtins, S. *J. Am. Chem. Soc.* **2004**, *126*, 16472.

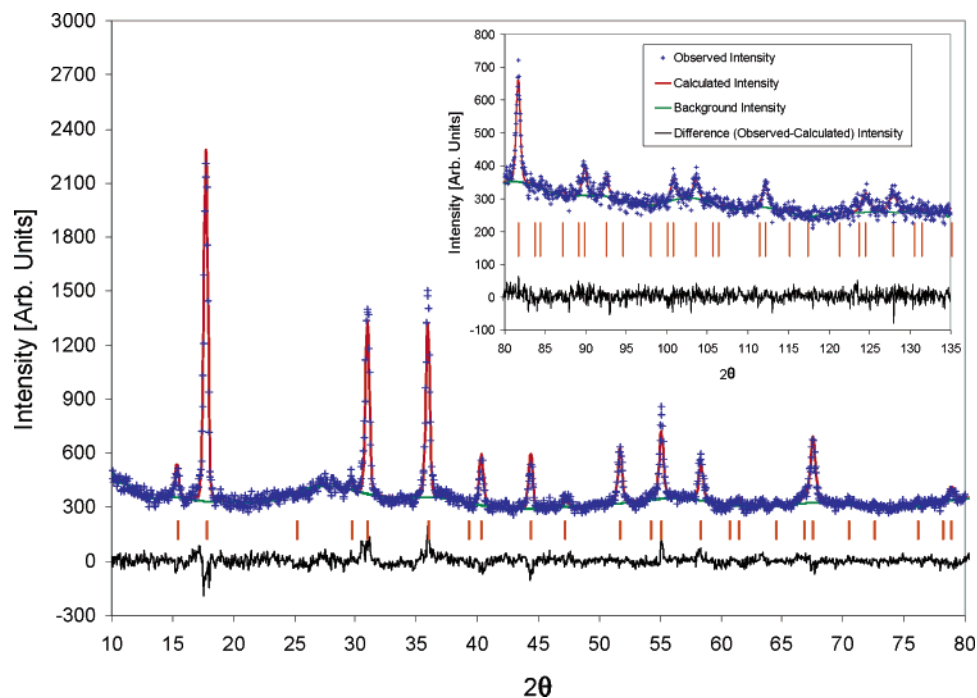


Figure 2. Results of the Rietveld refinement of the $\text{Cu}_3[\text{Co}(\text{CN})_6]_2$ with a hydrogen loading of 1 H_2/Cu .

Table 2. Summary of Rietveld Refinements of $\text{Cu}_3[\text{Co}(\text{CN})_6]_2$ with Various Hydrogen Loadings

Hydrogen loading [H_2/Cu]	lattice parameter, a [Å]	R_{wp}	R_{p}	DWd
0	10.0003(3)	0.0568	0.0461	1.221
1	10.0009(3)	0.0499	0.0406	1.242
2	10.0040(3)	0.0469	0.0369	1.428
2.3	10.0095(5)	0.0468	0.0366	1.327

hydrogen adsorption occurs at the $(x, 0, 0)$ sites. Gas adsorption at the $(\frac{1}{4}, \frac{1}{4}, \frac{1}{4})$ site has also previously been observed for the adsorption of nitrogen in this class of material.⁸

Each $(\frac{1}{4}, \frac{1}{4}, \frac{1}{4})$ site is surrounded by four $[\text{Co}(\text{CN})_6]^{3-}$ complexes, and these sites can be broadly classified by the number of $[\text{Co}(\text{CN})_6]^{3-}$ vacancies that exist adjacent to a particular site. Under the assumption that the $[\text{Co}(\text{CN})_6]^{3-}$ vacancies are aperiodic, the probability for a $(\frac{1}{4}, \frac{1}{4}, \frac{1}{4})$ site to be surrounded by a given number of vacancies, ranging from 0 to 4, can be treated as a binomial random variable. Table 4 summarizes the probabilities for the various types of sites and the corresponding hydrogen adsorption corresponding to a saturation of the site. From Table 3, the occupancy of the $(\frac{1}{4}, \frac{1}{4}, \frac{1}{4})$ site at the highest achievable hydrogen loading was 1.536(16), which suggests, based upon the information presented in Table 4, that the $(\frac{1}{4}, \frac{1}{4}, \frac{1}{4})$ sites with zero, one, or two adjacent $[\text{Co}(\text{CN})_6]^{3-}$ vacancies are suitable for hydrogen adsorption. At higher defect levels, the structure is sufficiently altered that the hydrogen molecules prefer to adsorb to the coordinatively unsaturated Cu^{2+} ions at the $(x, 0, 0)$ sites. The discrepancy between the amount of hydrogen admitted to the sample and that calculated based upon the Rietveld refinements provides a further indication that the sample contained some amorphous

material from the synthesis process or, alternatively, as a result of framework collapse during the evacuation of the sample.

The neutron vibrational spectroscopic features of $\text{Cu}_3[\text{Co}(\text{CN})_6]_2$ with several hydrogen loadings were observed on the FANS instrument. The raw data for each hydrogen loading were analyzed by subtracting the contribution from the evacuated material. The resulting spectra for a nominal hydrogen loading of 1/3, 1, and 2 H_2/Cu are shown in Figure 3. Both spectra exhibit similar features, but of particular note is the distribution of the spectra at about 14.7 meV (118.6 cm^{-1}). The first rotational transition for free hydrogen occurs at a value of 14.7 meV, and the fact that the observed spectra show split bands about this value is further indication that the hydrogen has been adsorbed to the framework structure. Similar splitting has also been recently observed in other nanoporous frameworks, namely, the metal–organic framework compounds.^{9,10} The broad features in the spectra suggest a range of local binding potentials for the adsorbed hydrogen, rather than one or two well-defined environments. This range in binding potentials can be ascribed to the variation in the potential induced by the different topologies of the $(\frac{1}{4}, \frac{1}{4}, \frac{1}{4})$ site and the corresponding variations in the $(x, 0, 0)$ site. Further computational efforts, currently underway, are needed to provide a further physical interpretation of the spectra.

Conclusions

Neutron powder diffraction, combined with Rietveld crystal refinement and difference Fourier techniques, has

(8) Chapman K. W.; Chupas P. J.; Kepert, C. J. *J. Am. Chem. Soc.* **2005**, *127*, 11232.

(9) Rosi, N. L.; Eckert, J.; Eddaoudi, M.; Vodak, D. T.; Kim, J.; O’Keeffe, M.; Yaghi, O. M. *Science* **2003**, *300*, 1127.
(10) Roswell, J. C.; Eckert, J.; Yaghi, O. M. *J. Am. Chem. Soc.* **2005**, *127*, 14904.

Table 3. Hydrogen Adsorption Site Characteristics as a Function of Hydrogen Loading

hydrogen loading [H ₂ /Cu]	(1/4, 1/4, 1/4) site fractional occupation ^a	(x, 0, 0) site location, x	(x, 0, 0) site fractional occupation ^a	hydrogen loading calculated from Rietveld refinement	
				[H ₂ /Cu]	[wt % H ₂]
1	1.102(25)	0.184(13)	0.126(32)	1.480(61)	1.4
2	1.424(16)	0.1995(22)	0.310(16)	2.254(32)	2.3
2.3	1.536(16)	0.2152(21)	0.430(17)	2.826(34)	2.7

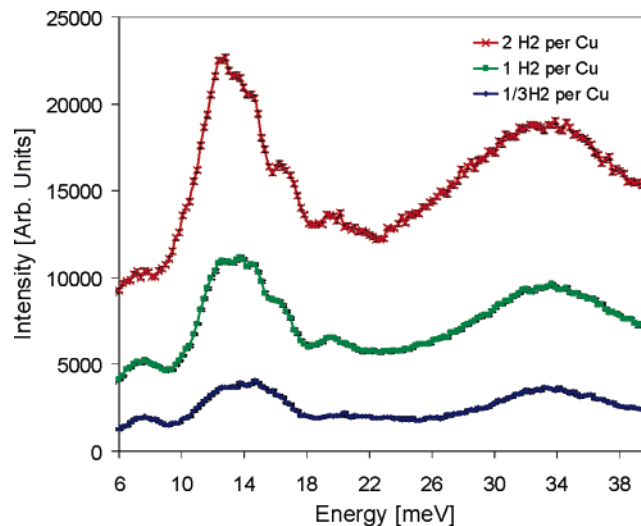
^a Saturation of the adsorption sites would correspond to a fractional occupation of 2 for the (1/4, 1/4, 1/4) site and 0.667 for the (x, 0, 0) site because molecular hydrogen contains two hydrogen atoms per molecule.

Table 4. Characterization of the (1/4, 1/4, 1/4) Adsorption Sites

number of adjacent [Co(CN) ₆] ³⁻ vacancies	frequency of occurrence	corresponding hydrogen adsorption at saturation [H ₂ /Cu]
0	0.1975	0.395
1	0.3951	0.790
2	0.2963	0.593
3	0.0988	0.198
4	0.0123	0.025

shown that hydrogen adsorption in the nanoporous Cu₃[Co(CN)₆]₂ Prussian blue analogue occurs at two crystallographic sites within the structure. One adsorption site, the (1/4, 1/4, 1/4) site, occurs at an interstitial location within the framework while the second adsorption site is situated on coordinatively unsaturated Cu²⁺ ions that result from the presence of [Co(CN)₆]³⁻ vacancies. The results show that Cu₃[Co(CN)₆]₂ is capable of storing ~2.7 wt % hydrogen at low temperatures.

Neutron vibrational spectroscopy measurements of Cu₃[Co(CN)₆]₂ at varying levels of hydrogen adsorption showed complex rotational transition bands, similar to what has been observed in other nanoporous framework materials.^{9,10} These broad features indicate a range of local bonding potentials for the adsorbed hydrogen molecules. This range of bonding potentials is attributed to the variations in the bonding sites that result from the local orientation of the [Co(CN)₆]³⁻ vacancies.

**Figure 3.** Neutron vibrational spectroscopy of Cu₃[Co(CN)₆]₂ with varying amounts of adsorbed hydrogen.

Acknowledgment. The authors wish to gratefully acknowledge the assistance of D. A. Neumann, T. J. Udovic, and J. Leão. This work was partially supported by the U.S. Department of Energy within the Center of Excellence on Carbon-based Hydrogen Storage Materials and by DOE No. DE-FG36-056015002. We thank the National Science Foundation for providing a predoctoral fellowship for S.S.K.

CM0608600